2D/3D One-Bit $\Sigma\Delta$ Modulation

Yisong Zhang†, Ayush Bhandari‡, Miguel Heredia Conde†
† Institute for High Frequency and Communication Technology, University of Wuppertal, Wuppertal, Germany
‡ Department of Electrical and Electronic Engineering, Imperial College London, London, U.K.
† {yzhang, herediaconde}@uni-wuppertal.de, ‡ a.bhandari@imperial.ac.uk

***Abstract*—This paper presents a novel framework for low-complexity, one-bit sigma-delta ($\Sigma\Delta$) modulation for two-dimensional (2D) and three-dimensional (3D) data, with applications in time-resolved imaging and data compression. We propose a 2D first-order $\Sigma\Delta$ scheme that quantizes bandlimited data into one-bit samples while shaping noise into unused high frequency bands. Extending this, we introduce a diagonal 2D model supporting both first-order (1st) and second-order (2nd) quantization, offering improved noise shaping and reconstruction accuracy. This model is further extended to 3D $\Sigma\Delta$ for volumetric and time-resolved data quantization. Leveraging oversampling, our method enables high-fidelity signal reconstruction. Experiments on 2D images, 3D synthetic data, and real Time-of-Flight (ToF) data validate our approach. We achieve successful data reconstruction from one-bit samples and practical utility in time-resolved imaging. Our results demonstrate significant data compression potentials, reducing storage and enhancing transfer speeds while preserving high reconstruction quality. This work bridges low-complexity data acquisition with high-quality reconstruction, paving the way for future research in megapixel-resolution time-resolved imaging and efficient data compression.**

***Index Terms*—One-bit sampling, Sigma-delta modulation, 2D, 3D, Time-resolved imaging, Data compression.**

I. Introduction

Time-resolved imaging (TRI) has emerged as a powerful tool in fields such as computational imaging, biomedical imaging, and 3D scene reconstruction, enabling the capture of scene-dependent time profiles at ultra-high temporal resolutions. However, the scalability of TRI systems is fundamentally limited by the need for high bit-rate analog-to-digital converters (ADCs), which increases hardware complexity and power consumption. To address this challenge, one-bit sampling [1] has gained attention as a low-complexity alternative, where measurements are quantized into binary values ($+1$ or -1). While one-bit sampling simplifies hardware design, it introduces significant information loss and poses unique challenges for signal reconstruction.

A key insight from existing $\Sigma\Delta$ modulation techniques is that oversampling can mitigate the effects of coarse quantization by shaping quantization noise into unused higher-frequency bands, allowing for effective reconstruction of bandlimited signals [2]. This principle has been widely leveraged in the temporal domain for time-resolved signals but remains underexplored for spatially structured data such as 2D images and 3D volumetric data. In particular, traditional one-bit $\Sigma\Delta$ methods [3]–[5] predominantly focus on 1D signal reconstruction in time-resolved imaging, overlooking the potential of extending noise shaping across spatial dimension.

Funded by the Deutsche Forschungsgemeinschaft (DFG, German Research Foundation) – 514479946.

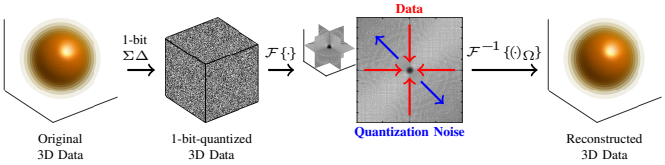

Fig. 1. Flowchart of the 1-bit quantization and reconstruction process for 3D data: Raw 3D data → 1-bit quantization → Low-pass filtering → Reconstructed 3D data.

Motivated by recent advances in Time-of-Flight (ToF) imaging, we highlight a crucial observation: as the ToF pixel pitch scales below twice the Airy disk radius given by $r_{Airy} = 1.22\frac{\lambda}{2NA}$, where λ is the wavelength of light and NA is the numerical aperture of the optical system, the bandlimited assumption holds not only in the temporal domain but also along spatial dimensions [6]. For example, modern ToF image sensors with $3\,\mu\mathrm{m}$ global shutter pixels [7] satisfy this condition for NA below approximately 0.2, assuming a typical ToF wavelength of $940\,\mathrm{nm}$, reinforcing the validity of bandlimited models in the spatial domain. This insight enables the application of $\Sigma\Delta$ modulation to 2D and 3D data, allowing for efficient one-bit quantization while exploiting spatial oversampling to improve reconstruction accuracy.

Building on this motivation, we propose a novel framework for low-complexity, one-bit $\Sigma\Delta$ modulation tailored for 2D and 3D data, with specific applications in time-resolved imaging and data compression. Fig. 1 is a schematic presentation of the proposed approach. Our contributions are as follows:

1) We introduce a 2D 1st-order $\Sigma\Delta$ modulation scheme, which quantizes 2D data into one-bit samples.
2) We develop a diagonal 2D model that supports both 1st-order and 2nd-order quantization, offering improved noise shaping and reconstruction accuracy.
3) We extend this diagonal model to 3D $\Sigma\Delta$ modulation, enabling efficient quantization and reconstruction of volumetric and time-resolved data.
4) We validate our approach through extensive experiments on 2D images, 3D synthetic data, and real Time-of-Flight (ToF) data [8], demonstrating its practical utility in time-resolved imaging and data compression.

Our results demonstrate that the proposed method achieves high-fidelity reconstruction from one-bit samples, and offers

significant potential for data compression by reducing storage requirements and increasing data transfer efficiency. By bridging the gap between low-complexity data acquisition and high-quality reconstruction, this work paves the way for future research in megapixel-resolution time-resolved imaging and efficient data compression.

II. Methodology

This section presents the mathematical formulation of the proposed 2D and 3D one-bit $\Sigma\Delta$ modulation schemes, building on the foundational principles of 1D one-bit sampling [9] as described in prior work [10]. In 1D $\Sigma\Delta$ modulation, a continuous-time signal $f(t)$ is quantized into one-bit samples $q[n] \in \{-1, +1\}$ using a recursive feedback loop:

$$q[n] = \text{sgn}(u[n-1] + f[n]) \tag{1}$$
$$u[n] = u[n-1] + f[n] - q[n] \tag{2}$$

where $u[n]$ is the state variable, and the quantization error is shaped into higher frequencies through a finite difference operator. This approach has been widely used in reconstruction of bandlimited ToF data [3] and low-complexity data acquisition. However, extending this framework to multidimensional data (e.g., 2D images and 3D volumetric data) introduces new challenges, particularly in managing quantization noise and ensuring accurate reconstruction.

While 2D generalizations of $\Sigma\Delta$ modulation have been explored in previous works [11]–[13], they primarily focus on specific architectures or limited noise-shaping strategies. In this work, we extend the 1D $\Sigma\Delta$ modulation framework to 2D and 3D domains by introducing novel quantization schemes that leverage recursive state updates and noise shaping to achieve high-fidelity reconstruction. Below, we detail the mathematical formulation of our proposed methods, beginning with 2D 1st-order $\Sigma\Delta$ modulation, followed by a diagonal 2D model that supports both 1st-order and 2nd-order quantization, and finally extending these concepts to 3D $\Sigma\Delta$ modulation.

A. 2D 1st-order $\Sigma\Delta$ Modulation

Let $f[i, j]$ represent the input 2D discrete signal (e.g., an image) at pixel coordinates (i, j). The quantization process is defined as:

$$q[i, j] = \text{sgn}(c_0 u[i-1, j] + c_1 u[i, j-1] + f[i, j]) \tag{3}$$

where $q[i, j] \in \{-1, +1\}$ is the one-bit quantized output, and $u[i, j]$ is the state variable updated recursively as:

$$u[i, j] = u[i-1, j] + u[i, j-1] - u[i-1, j-1] + f[i, j] - q[i, j] \tag{4}$$

Here, c_0 and c_1 are weighting coefficients that control the contribution of the neighboring state variables $u[i-1, j]$ and $u[i, j-1]$. This recursive update ensures that the quantization error $f[i, j] - q[i, j]$ is fed back into the system, effectively pushing the noise into higher frequencies.

B. Diagonal 2D $\Sigma\Delta$ Modulation

To reduce the complexity of the model, enhance noise shaping, and improve reconstruction accuracy, we propose a diagonal 2D $\Sigma\Delta$ modulation model that supports both 1st-order and 2nd-order quantization. Let $f[i, j]$ represent the input 2D signal at pixel coordinates (i, j).

For the 1st-order case, the quantization process is defined as:

$$q[i, j] = \text{sgn}(u[i-1, j-1] + f[i, j]) \tag{5}$$

where $q[i, j] \in \{-1, +1\}$ is the one-bit quantized output, and $u[i, j]$ is the state variable updated recursively as:

$$u[i, j] = u[i-1, j-1] + f[i, j] - q[i, j] \tag{6}$$

For the 2nd-order case, we introduce an additional state variable $x[i, j]$ to further suppress quantization noise. The 2nd-order quantization is defined as:

$$q^{[2]}[i, j] = \text{sgn}(c_0 u[i-1, j-1] + x[i-1, j-1] + f[i, j]) \tag{7}$$

where c_0 is a constant parameter (typically $c_0 = 0.5$). The state variables $u[i, j]$ and $x[i, j]$ are updated as:

$$u[i, j] = u[i-1, j-1] + x[i, j] \tag{8}$$
$$x[i, j] = x[i-1, j-1] + f[i, j] - q^{[2]}[i, j]. \tag{9}$$

This 2nd-order scheme provides better noise shaping, particularly in scenarios with high dynamic range or noisy input signals [9].

C. Extension to 3D $\Sigma\Delta$ Modulation

We extend the diagonal 2D model to 3D $\Sigma\Delta$ modulation to handle volumetric or time-resolved data. Let $f[i, j, k]$ represent the input 3D discrete signal at coordinates (i, j, k). The 1st-order 3D quantization is defined as:

$$q[i, j, k] = \text{sgn}(u[i-1, j-1, k-1] + f[i, j, k]) \tag{10}$$

with the state variable $u[i, j, k]$ updated as:

$$u[i, j, k] = u[i-1, j-1, k-1] + f[i, j, k] - q[i, j, k]. \tag{11}$$

For the 2nd-order 3D quantization, we introduce an additional state variable $x[i, j, k]$, and the $\Sigma\Delta$ quantization is defined as:

$$\begin{aligned} q^{[2]}[i, j, k] = \text{sgn}(&c_0 u[i-1, j-1, k-1] \\ &+ x[i-1, j-1, k-1] + f[i, j, k]) \end{aligned} \tag{12}$$

with the state variables updated as:

$$u[i, j, k] = u[i-1, j-1, k-1] + x[i, j, k] \tag{13}$$
$$x[i, j, k] = x[i-1, j-1, k-1] + f[i, j, k] - q^{[2]}[i, j, k].$$

This 3D extension enables efficient quantization of volumetric data while maintaining the noise-shaping properties.

D. Reconstruction from One-Bit Samples

The original bandlimited 2D/3D discrete signal is reconstructed from its one-bit quantized samples by leveraging low-pass filtering in the Fourier domain to suppress quantization noise while preserving the essential signal components. Let the Fourier transform of the one-bit samples be denoted by:

$$Q[\boldsymbol{\omega}] = \mathcal{F}\{q[\mathbf{x}]\}, \tag{14}$$

where $q[\mathbf{x}]$ is the one-bit quantized signal, $\mathbf{x} = (i, j)$ for 2D spatial data or $\mathbf{x} = (i, j, k)$ for 3D spatiotemporal data, $\boldsymbol{\omega} = (\omega_1, \omega_2)$ or $\boldsymbol{\omega} = (\omega_1, \omega_2, \omega_3)$, respectively.

Since the original signal is bandlimited, only frequencies within a known 2D/3D region Ω_{band} contain valid information, a low-pass filter is applied in the Fourier domain to retain these components:

$$\tilde{Q}[\boldsymbol{\omega}] = H[\boldsymbol{\omega}]Q[\boldsymbol{\omega}], \tag{15}$$

where the filter $H[\boldsymbol{\omega}]$ is defined as:

$$H[\boldsymbol{\omega}] = \begin{cases} 1, & \boldsymbol{\omega} \in \Omega_{\text{band}} \\ 0, & \text{otherwise} \end{cases} \tag{16}$$

After filtering, the signal is reconstructed by applying the inverse Fourier transform:

$$\tilde{f}[\mathbf{x}] = \mathcal{F}^{-1}\{\tilde{Q}[\boldsymbol{\omega}]\} \tag{17}$$

This recovers a bandlimited approximation $\tilde{f}[\mathbf{x}]$ of the original signal $f[\mathbf{x}]$, with minimal reconstruction error:

$$\arg\min_{\tilde{f} \in \Sigma_{\Omega_{\text{band}}}} \sum_{n=0}^{N-1} \left| \tilde{f}[n] - f[n] \right|^2 < \varepsilon \tag{18}$$

where $\tilde{f}[n]$ and $f[n]$ denote spatial sample points of the reconstructed and original signals, respectively, $\Sigma_{\Omega_{\text{band}}}$ the set of Ω_{band}-bandlimited signals and N the number of samples.

E. Oversampling and Noise Shaping

The performance of the proposed method depends on the oversampling factor μ and the order of quantization [10]. Higher oversampling factors and higher-order quantization schemes improve noise shaping and reconstruction accuracy. The reconstruction error [10] is bounded by $\left| f[i,j] - \tilde{f}[i,j] \right| \leq \frac{1}{\mu^L} \left\| \varphi^{(L)} \right\|_{L_1}$, where L is the order of quantization, μ is the oversampling factor, and $\varphi^{(L)}$ is the interpolation kernel.

This bound ensures that the reconstruction error decreases exponentially with increasing μ and L.

In the current implementation, oversampling in the spatial domain is simulated via interpolation methods. However, as the pixel pitch of ToF pixels decreases below the point spread function (PSF) of the lens, optical oversampling will naturally occur. Further oversampling can be achieved using optical techniques such as spatial light modulators (SLMs) [14] or diffractive optical elements (DOEs) [15], which can physically enhance the spatial resolution of the imaging system [16].

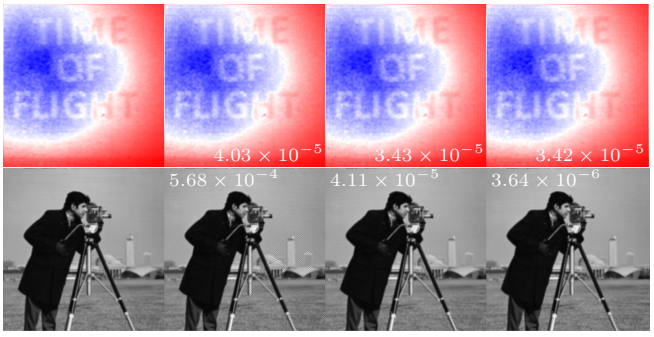

Fig. 2. (a) The ground truth of "TIME OF FLIGHT" image [3] and Cameraman image. (b)-(d) Recovered images from standard 1st-order, diagonal 1st-order, and diagonal 2nd-order one-bit samples, respectively. The MSE between the reconstructed images and the ground truth is shown in the image.

III. Experimental Evaluation

This section presents the experimental validation of the proposed 2D and 3D one-bit $\Sigma\Delta$ modulation schemes. We evaluate the performance of our methods on 2D images, 3D synthetic data, and real ToF data [8], demonstrating their effectiveness in signal reconstruction, noise shaping, and parametric depth and amplitude estimation. The experiments are divided into three parts: (1) 2D image reconstruction, (2) 3D synthetic data reconstruction, and (3) real ToF data analysis. For each experiment, we provide details on the dataset, experimental setup, and results.

A. 2D Image Reconstruction

Dataset. We tested the standard 2D 1st-order and proposed diagonal 2D $\Sigma\Delta$ modulation schemes on two images: the "TIME OF FLIGHT" amplitude image [3] and the Cameraman image [17]. These images were chosen for their varying textures and complexity, making them suitable for evaluating the robustness of the quantization and reconstruction processes.

Experimental Setup. Quantization: The images were quantized using the 1st-order and 2nd-order diagonal 2D $\Sigma\Delta$ modulation schemes. Oversampling: In the spatial domain, oversampling was simulated by applying linear interpolation with a factor of 50, followed by low-pass filtering to suppress high-frequency artifacts and ensure bandlimiting. Reconstruction: The original images were reconstructed from the one-bit samples using the frequency-domain reconstruction method described in Section II-D. Fourier Spectrum Analysis: The Fourier spectrum of the one-bit samples was analyzed to demonstrate the compression of the signal into a limited bandwidth and the shaping of noise into higher frequencies.

Results. Reconstruction Quality: As shown in Fig. 2, the reconstruction results from the standard 2D 1st-order method, the diagonal 2D 1st-order method, and the diagonal 2D 2nd-order method were visually indistinguishable from the original images for both the "TIME OF FLIGHT" image and the Cameraman image. This demonstrates the effectiveness of the proposed methods in preserving image details.

Fourier Spectrum: As shown in Fig. 3(a)-3(f), the Fourier spectrum of the one-bit samples demonstrates that the signal

is confined within a limited bandwidth, while quantization noise is pushed to higher frequencies. Additionally, the diagonal methods further suppress quantization error, reducing it to nearly zero along the direction of quantizer operation. This confirms the noise-shaping capabilities of the proposed method.

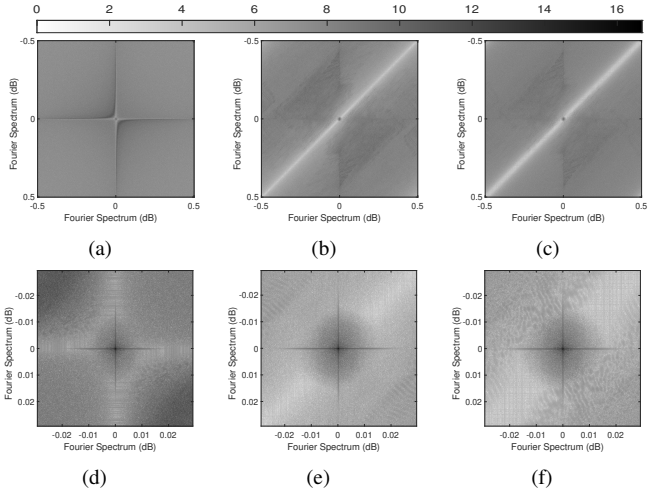

Fig. 3. Fourier spectrum (dB) of one-bit sampling results. (a) Standard 2D 1st-order result, (b) Diagonal 2D 1st-order result, (c) Diagonal 2D 2nd-order result. (d)-(f) Zoomed-in low-frequency regions of (a)-(c), respectively.

Quantization Error: The mean squared error (MSE) between the original and reconstructed images was calculated using $\text{MSE}(\tilde{f}, f) = \frac{1}{N}\sum_{n=0}^{N-1}\left|\tilde{f}[n] - f[n]\right|^2$.

As shown in Table I, the 2nd-order scheme achieves a lower MSE compared to the 1st-order scheme. Moreover, our proposed "diagonal simplification" model not only preserves reconstruction accuracy but also improves it.

TABLE I
QUANTIZATION ERROR OF 2D ΣΔ MODULATIONS

Dataset	*Standard 1st-order*	*Diagonal 1st-order*	*Diagonal 2nd-order*
TOF*	4.03×10^{-5}	3.43×10^{-5}	3.42×10^{-5}
Cameraman	5.68×10^{-4}	4.11×10^{-5}	3.64×10^{-6}

*"TIME OF FLIGHT" image.

B. 3D Synthetic Data Reconstruction

Dataset. We generated a synthetic 3D dataset consisting of a Gaussian sphere to evaluate the performance of the proposed 3D ΣΔ modulation scheme in handling volumetric data. The dataset was created by defining a 3D grid with coordinates ranging from -1 to 1 along the x, y, and z axes, with a resolution of 800 points per axis. A Gaussian function with a standard deviation of $\sigma = 0.2$ was evaluated on the grid to create a 3D sphere centered at the origin. The intensity of the sphere decays exponentially with distance from the center, simulating a soft spherical object with a smooth intensity profile.

Experimental Setup. The experimental setup for 3D data follows the same methodology as the 2D case, utilizing the 1st-order and 2nd-order diagonal 3D ΣΔ modulation schemes. In this setup, the sampling rate exceeds the Nyquist rate by a factor of 38.

Results. Reconstruction Quality: As shown in Fig. 4(a)-4(c), the 3D Gaussian sphere was perfectly reconstructed from the one-bit samples, with no visible artifacts or distortions.

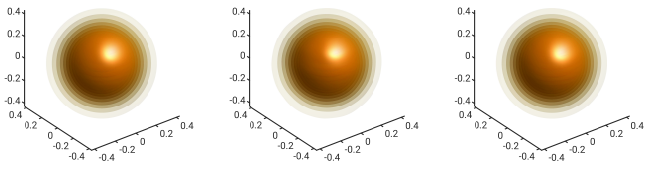

Fig. 4. (a) Original 3D Gaussian sphere. (b) Recovered 3D Gaussian sphere from diagonal 3D 1st-order one-bit samples. (c) Recovered 3D Gaussian sphere from diagonal 3D 2nd-order one-bit samples.

Fourier Spectrum: For the 1st-order scheme, the full spectrum Fig. 5(a) and its slices in the spatial and time domains Fig. 5(b)-5(d) show that the signal is confined to a limited bandwidth while quantization noise is pushed to higher frequencies, whereas for the 2nd-order scheme, Fig. 5(e) and Fig. 5(f)-5(h) demonstrate stronger noise shaping, further refining the bandwidth with minimal residual noise, as evident from the central black circular area representing signal components and the white region indicating a clean band.

Quantization Error: The mean squared error (MSE) between the original and reconstructed 3D sphere was calculated. The 1st-order scheme achieved an MSE of 3.22×10^{-5}, while the 2nd-order scheme achieved a significantly lower MSE of 6.37×10^{-7}. This demonstrates the superior noise-shaping capabilities of the 2nd-order scheme.

TABLE II
DATA SIZE COMPARISON (BYTES)

Dataset	*Original*	*Compressed*	*Ratio (≈)*
TOF*	2.8×10^8	1.6×10^5	1750 : 1
Cameraman	2.3×10^8	6.5×10^5	354 : 1
Gaussian Sphere	4.1×10^9	1.5×10^5	27333 : 1

*"TIME OF FLIGHT" image.

C. Real Time-of-Flight Data Analysis

Dataset. We used real ToF raw data obtained by observing a diffusive, semitranslucent sheet that covers a placard reads "TIME OF FLIGHT" [8]. The dataset consists of raw coded ToF data acquired at different time shifts.

Experimental Setup. Quantization: The ToF data was quantized using the diagonal 3D ΣΔ modulation schemes. Oversampling: Oversampling in the spatial domain was simulated by applying linear interpolation with a factor of 6. Reconstruction: The original ToF data was reconstructed from the one-bit samples using the frequency-domain reconstruction method in (15)-(17). Depth and Amplitude Estimation: The matrix pencil method [18] was applied to time-domain Fourier samples of the reconstructed signal to parametrically estimate depth and amplitude information, following the approach in [3].

Results. Depth and Amplitude Accuracy: As shown in Fig. 6, the estimated depth and amplitude values were compared to the ground truth. The results were encouraging but also revealed slight distortion, indicating room for improvement.

D. Discussion

The proposed 2D and 3D one-bit ΣΔ modulation schemes achieve high-fidelity reconstruction, with 2nd-order schemes

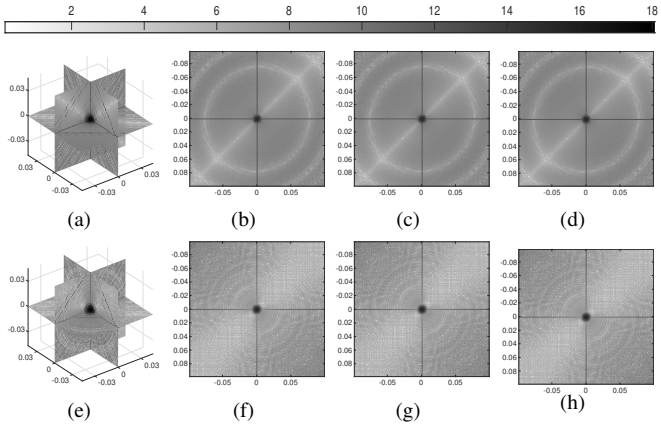

Fig. 5. Fourier spectrum (dB) analysis of the 3D Gaussian sphere. Zoomed-in low-frequency regions of (a) Full spectrum from 3D 1st-order one-bit samples. (b)-(d) Slices of the spectrum from 3D 1st-order samples in spatial and time domains. (i) Full spectrum from 3D 2nd-order one-bit samples. (j)-(l) Slices of the spectrum from 3D 2nd-order samples in spatial and time domains.

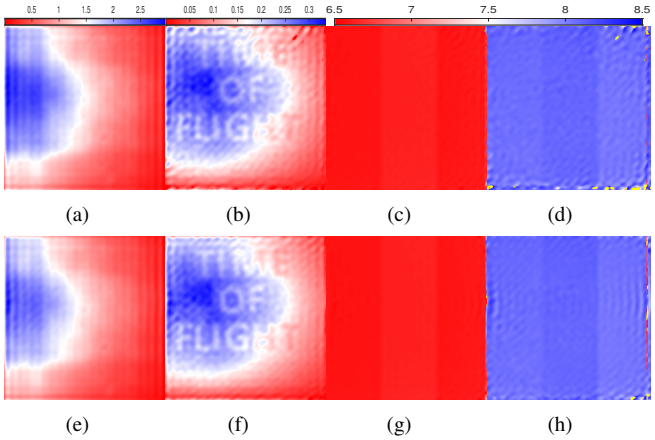

Fig. 6. Estimated amplitude (a.u.) and depth (m) from 3D one-bit samples. (a)-(b) Amplitude from 3D 1st-order samples for two scenes. (c)-(d) Depth from 3D 1st-order samples for two scenes. (e)-(f) Amplitude from 2nd-order samples. (g)-(h) Depth from 2nd-order samples.

demonstrating superior noise shaping and accuracy, particularly in challenging conditions. As shown in Table II, the compressed bandlimited Fourier spectrum of one-bit samples, which enables accurate reconstruction, is significantly smaller than the original data, highlighting the method's potential for efficient data compression across various datasets.

IV. Conclusion

In this paper, we proposed a novel framework for low-complexity, one-bit $\Sigma\Delta$ modulation applied to 2D and 3D data, with applications in time-resolved imaging and data compression. Our work makes the following key contributions. 2D 1st-order $\Sigma\Delta$ modulation: we presented a 2D 1st-order $\Sigma\Delta$ modulation scheme and developed simplified versions of the quantizers offering improved noise shaping and reconstruction accuracy. 3D extension: we extended the diagonal 2D model to 3D $\Sigma\Delta$ modulation, enabling efficient quantization and reconstruction of volumetric and time-resolved data. Our work bridges the gap between low-complexity data acquisition and high-quality reconstruction, offering a promising direction for future research in megapixel-resolution time-resolved imaging and efficient data compression. The proposed methods are particularly well-suited for applications in computational 3D imaging, LiDAR systems [19], and real-time data processing.

Future research directions include: a) Comprehensive noise robustness evaluation, improving the robustness of the proposed methods to real-world noise and model mismatch, particularly in time-resolved imaging applications. b) Hardware implementation, including the development of efficient on-chip implementations of the proposed quantization.

References

[1] P. M. Aziz, H. V. Sorensen, and J. vn der Spiegel, "An overview of sigma-delta converters," *IEEE signal processing magazine*, vol. 13, no. 1, pp. 61–84, 1996.

[2] S. Pavan, R. Schreier, and G. C. Temes, *Understanding delta-sigma data converters*. John Wiley & Sons, 2017.

[3] A. Bhandari, M. Heredia Conde, and O. Loffeld, "One-bit time-resolved imaging," *IEEE Trans. on Patt. Anal. and Mach. Intell.*, vol. 42, no. 7, pp. 1630–1641, 2020.

[4] P. T. Boufounos and R. G. Baraniuk, "1-bit compressive sensing," in *2008 42nd Annual Conference on Information Sciences and Systems*. IEEE, 2008, pp. 16–21.

[5] Z. Li, W. Xu, X. Zhang, and J. Lin, "A survey on one-bit compressed sensing: Theory and applications," *Frontiers of Computer Science*, vol. 12, pp. 217–230, 2018.

[6] M. Heredia Conde, K. Hartmann, and O. Loffeld, "Subpixel spatial response of PMD pixels," in *2014 IEEE International Conference on Imaging Systems and Techniques (IST) Proceedings*. IEEE, 2014, pp. 297–302.

[7] C. S. Bamji, S. Mehta, B. Thompson, T. Elkhatib, S. Wurster, O. Akkaya, A. Payne, J. Godbaz, M. Fenton, V. Rajasekaran *et al.*, "IMpixel 65nm BSI 320MHz demodulated TOF Image sensor with $3\mu m$ global shutter pixels and analog binning," in *2018 IEEE International Solid-State Circuits Conference-(ISSCC)*. IEEE, 2018, pp. 94–96.

[8] A. Bhandari and R. Raskar, "Signal processing for time-of-flight imaging sensors: An introduction to inverse problems in computational 3-D imaging," *IEEE Signal Processing Magazine*, vol. 33, no. 5, pp. 45–58, 2016.

[9] C. Güntürk, "Approximating a bandlimited function using very coarsely quantized data: improved error estimates in sigma-delta modulation," *Journal of the American Mathematical Society*, vol. 17, no. 1, pp. 229–242, 2004.

[10] I. Daubechies and R. DeVore, "Approximating a bandlimited function using very coarsely quantized data: A family of stable sigma-delta modulators of arbitrary order," *Annals of mathematics*, vol. 158, no. 2, pp. 679–710, 2003.

[11] S. Handagala, A. Madanayake, L. Belostotski, and L. T. Bruton, "Delta-sigma noise shaping in 2D spacetime for uniform linear aperture array receivers," in *2016 Moratuwa Engineering Research Conference (MERCon)*. IEEE, 2016, pp. 114–119.

[12] T. D. Kite, B. L. Evans, A. C. Bovik, and T. L. Sculley, "Digital halftoning as 2-D delta-sigma modulation," in *Proceedings of International Conference on Image Processing*, vol. 1. IEEE, 1997, pp. 799–802.

[13] H. Aomori, T. Otake, N. Takahashi, and M. Tanaka, "Sigma–delta cellular neural network for 2D modulation," *Neural networks*, vol. 21, no. 2-3, pp. 349–357, 2008.

[14] D. G. Grier, "A revolution in optical manipulation," *Nature*, vol. 424, no. 6950, pp. 810–816, 2003.

[15] A. Ozcan and U. Demirci, "Ultra wide-field lens-free monitoring of cells on-chip," *Lab on a Chip*, vol. 8, no. 1, pp. 98–106, 2008.

[16] J. W. Goodman, *Introduction to Fourier optics*. Roberts and Company publishers, 2005.

[17] M. R. Banham and A. K. Katsaggelos, "Digital image restoration," *IEEE signal processing magazine*, vol. 14, no. 2, pp. 24–41, 1997.

[18] Y. Hua and T. K. Sarkar, "Matrix pencil method for estimating parameters of exponentially damped/undamped sinusoids in noise," *IEEE Transactions on Acoustics, Speech, and Signal Processing*, vol. 38, no. 5, pp. 814–824, 1990.

[19] S. Hernández-Marín, A. M. Wallace, and G. J. Gibson, "Bayesian analysis of lidar signals with multiple returns," *IEEE Trans. on Patt. Anal. and Mach. Intell.*, vol. 29, no. 12, pp. 2170–2180, 2007.